Single excitation energies obtained from the ensemble HOMO-LUMO gap: exact results and approximations

Tim Gould,*,† Zahed Hashimi,† Leeor Kronik,‡ and Stephen Dale†

†*Qld Micro- and Nanotechnology Centre, Griffith University, Nathan, Qld 4111, Australia*

‡*Department of Molecular Chemistry and Materials Science, Weizmann Institute of Science, Rehovoth 76100, Israel*

E-mail: t.gould@griffith.edu.au

Abstract

In calculations based on density functional theory, the "HOMO-LUMO gap" (difference between the highest occupied and lowest unoccupied molecular orbital energies) is often used as a low-cost, *ad hoc* approximation for the lowest excitation energy. Here we show that a simple correction based on rigorous ensemble density functional theory makes the HOMO-LUMO gap exact, in principle, and significantly more accurate, in practice. The introduced perturbative ensemble density functional theory approach predicts different and useful values for singlet–singlet and singlet–triplet excitations, using semi-local and hybrid approximations. Excitation energies are of similar quality to time-dependent density functional theory, especially at high fractions of exact exchange. It therefore offers an easy-to-implement and low-cost route to robust prediction of molecular excitation energies.

TOC Graphic

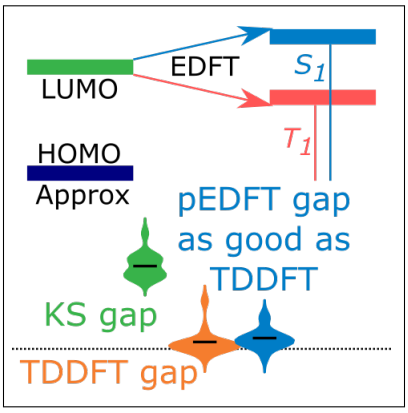

Ground state calculations based on density functional theory[1,2] (DFT) have transformed chemical understanding and are increasingly used in a predictive fashion, owing to the availability of high quality density functional approximations (DFAs) that can be used at a relatively low computational cost.[3–7] The prediction of excited state properties is also of much importance and is usually addressed using time-dependent DFT (TDDFT).[8–12] Recently, ensemble DFT (EDFT)[13,14] is being increasingly explored[15–30] as a promising alternative to TDDFT for low-cost quantitative prediction of excitation energies.

Of particular importance is the lowest excitation energy, often referred to as the optical gap.[9,31] The DFT "HOMO-LUMO gap", defined as $\epsilon_l - \epsilon_h$, where ϵ indicates an orbital energy, h indicates the highest occupied molecular orbital (HOMO), and l the lowest unoccupied molecular orbital (LUMO) is often used as a rough, computationally inexpensive approximation to the optical gap,[9,31] with some approximate argumentation [32,33] but no rigorous justification. In this work we first show that a carefully defined HOMO-LUMO gap within EDFT *exactly* yields the lowest lying excitation energy. Furthermore, this exact relation applies to both triplet and singlet excitations, and can be used with both traditional and hybrid density functional approximations (DFAs). We then show that using common DFAs, this relation leads to results of similar quality to those of TDDFT. The EDFT gap therefore energes as a low-cost, useful approach to the quantitative prediction of the lowest excitations.

We begin our considerations by briefly reviewing pertinent issues in DFT and EDFT. Conventional, pure state DFT expresses the electronic ground state energy, E_0, as $E_0 = \langle\Psi|\hat{H}|\Psi\rangle = T_s[n] + E_{\text{Hxc}}[n] + \int n(\boldsymbol{r})v(\boldsymbol{r})d\boldsymbol{r}$, where Ψ is the many-electron ground-state wave function, $\hat{H}$ is the many-electron Hamiltonian, T_s is the non-interacting kinetic energy, E_{Hxc} in the Hartree-exchange-correlation (Hxc) energy, v is the external potential, and n is the electron density. The difficult many-body problem may then be replaced by the simpler problem of finding a set of one-body orbitals, $\{\phi_i\}$ (elaborated below), from which one obtains the density, $n = \sum_{i\in\text{occ}} |\phi_i|^2$, as well as T_s. A DFA captures the requisite quantum

mechanics by approximating E_{Hxc}.

EDFT for excited states[13,14] generalizes DFT to a statistical average across multiple states, $\mathcal{E}^{\mathbf{w}} = \sum_\kappa w_\kappa \langle \Psi_\kappa | \hat{H} | \Psi_\kappa \rangle = \text{Tr}[\hat{\Gamma}^{\mathbf{w}} \hat{H}]$, where Ψ_κ is the many-electron wave function associated with a specific energy level, κ, $w_\kappa \geq 0$ is the weight assigned to that energy level, and $\hat{\Gamma} = \sum_\kappa w_\kappa |\Psi_\kappa\rangle\langle\Psi_\kappa|$ is an ensemble density matrix. Conventional DFT is then the special case $w_0 = 1$ and $w_{\kappa>0} = 0$. The relevant density is $n^{\mathbf{w}} = \sum_\kappa w_\kappa \langle \Psi_\kappa | \hat{n} | \Psi_\kappa \rangle = \sum_i f_i^{\mathbf{w}} |\phi_i|^2$, where $f_i^{\mathbf{w}}$ are effective occupation factors that depend on the weights. Standard DFT machinery may be adapted to ensembles,[13,14,19,21–24] yielding $\mathcal{E}^{\mathbf{w}} = \mathcal{T}_s^{\mathbf{w}}[n^{\mathbf{w}}] + \mathcal{E}_{\text{Hxc}}^{\mathbf{w}}[n^{\mathbf{w}}] + \int n^{\mathbf{w}}(\boldsymbol{r}) v(\boldsymbol{r}) d\boldsymbol{r}$ for a given ensemble state, and therefore $\mathcal{E}^{\mathbf{w}} \approx \mathcal{T}_s^{\mathbf{w}}[n^{\mathbf{w}}] + \mathcal{E}_{\text{Hxc}}^{\text{EDFA},\mathbf{w}}[n^{\mathbf{w}}] + \int n^{\mathbf{w}}(\boldsymbol{r}) v(\boldsymbol{r}) d\boldsymbol{r}$ for an ensemble state obtained using a given DFA, where $\mathcal{T}_s$ is the ensemble non-interacting kinetic energy and $\mathcal{E}_{\text{Hxc}}$ is the ensemble Hxc energy. Excited state energies may then be computed via $E_\kappa := \frac{\partial \mathcal{E}^{\mathbf{w}}}{\partial w_\kappa}$, or other formulae.[25,28] EDFAs may thereby be used to predict properties of non-trivial excited states.

A typical practical DFT calculation involves finding orbitals, $\{\phi_i\}$, and orbital energies, ϵ_i, obeying the (original[2] or generalized[34]) Kohn-Sham (KS) equation, $\hat{h}\phi_i = \{\hat{h}_0 + \hat{v}_{\text{Hxc}}[n]\}\phi_i = \epsilon_i \phi_i$. Here, $\hat{h}_0 = -\frac{1}{2}\nabla^2 + v$ contains the one-body kinetic energy operator and nuclear potential, v. The Hxc potential, $\hat{v}_{\text{Hxc}}[n]$, maps the many-electron interactions to the one-body Hamiltonian. It may depend on spin (in an unrestricted Kohn-Sham formalism) and/or be non-multiplicative (in the generalized KS approach). All formalisms can be made exact, in the DFT sense of yielding the exact density and energy, for pure and degenerate ground states.[2,24,34,35] Moreover, in *any* exact calculation of a molecule, the HOMO eigenvalue, ϵ_h, is the negative of the ionization potential (IP) of the system.[35–39] This relationship is often known as the "IP theorem".

In practice, $\hat{v}_{\text{Hxc}}[n] \approx \hat{v}_{\text{Hxc}}^{\text{DFA}}$ is obtained from a DFA and the resulting orbital energy, ϵ_h^{DFA}, does not necessarily come even close to satisfying the IP theorem.[40] Kraisler and Kronik showed[41–43] that agreement between ϵ_h^{DFA} and IP^{DFA} could be improved at essentially no cost by invoking exact relationships from ensembles with non-integer numbers of electrons.[36]

This begs the question of whether similar improvements can be made to the HOMO-LUMO gap by invoking exact results for excited-state ensembles. We proceed to reveal that this is indeed the case, by first deriving an exact relationship [eq. (1)] and then demonstrating that the resulting formalism improves the quality of excitations found in practice using common DFAs.

Like their conventional DFT counterparts, EDFT orbitals obey effective one-body ensemble GKS (EGKS) equations,[24] $[\hat{h}_0 + \hat{v}^{\mathbf{w}}_{\mathrm{Hxc},i}]\phi^{\mathbf{w}}_i = \epsilon^{\mathbf{w}}_i \phi^{\mathbf{w}}_i + \sum_{j\neq i} \varepsilon^{\mathbf{w}}_{ij}\phi^{\mathbf{w}}_j$. Here, a crucial difference from conventional DFT is that the effective potential $\hat{v}^{\mathbf{w}}_{\mathrm{Hxc},i}$ can depend on the orbital label, i. Thus, Lagrange multipliers, ε_{ij}, can be required to ensure orthonormality, $\int \phi^*_i(\boldsymbol{r})\phi_j(\boldsymbol{r})d\boldsymbol{r} = \delta_{ij}$. Despite additional practical complexities, EDFT for excited states can also be made exact in the same sense as its pure state counterpart.[13,14,19,24]

We now restrict ourselves to the important problem of finding the lowest excitations in a system. We illustrate our approach using the case of a singlet ground state, but most results can be generalized. We have three states of interest: the ground state (gs) $|S_0\rangle = |1^2 \cdots h^2\rangle$, and singly excited states (sx, $h \to l$) $|T_1\rangle = |1^2 \cdots h^\uparrow l^\uparrow\rangle$ (the triplet is degenerate in EDFT[19] so we can equivalently choose one of the other two options) and $|S_1\rangle = \frac{1}{\sqrt{2}}[|1^2 \cdots h^\uparrow l^\downarrow\rangle + |1^2 \cdots h^\downarrow l^\uparrow\rangle]$. The core theory behind our approach may be summarised by the following exact relationships:

1. The energy of the HOMO of the ground state (S_0) GKS state is the ionisation potential of the system, i.e., $\epsilon^{S_0}_h = E^{\mathrm{sys}}_{\mathrm{gs}} - E^{\mathrm{sys}^+}_{\mathrm{gs}}$;[35–37,39,44,45]

2. The energy of the highest occupied orbital of any singly-excited (sx $\in \{T_1, S_1\}$) GKS state is given by $\epsilon^{\mathrm{sx}}_l = E^{\mathrm{sys}}_{\mathrm{sx}} - E^{\mathrm{sys}^+}_{\mathrm{gs}}$;[46]

3. The energy of the highest occupied orbital of an EGKS system, $\hat{\Gamma}^w = (1-w)|S_0\rangle\langle S_0| + w|\mathrm{sx}\rangle\langle\mathrm{sx}|$ is equal to that of the sx, $\epsilon^{\mathrm{ens}}_l = \epsilon^{\mathrm{sx}}_l = E^{\mathrm{sys}}_{\mathrm{sx}} - E^{\mathrm{sys}^+}_{\mathrm{gs}}$.

All three follow from fundamental relationships between energy differences and the asymptotic behaviour of electronic densities.[44,46] The final relationship may be new to this work,

and can be derived using similar arguments to Perdew *et al*[36] or Gould *et al.*[39] Details are provided in Section 1 of the Supporting Information (SI).

The consequence of the three relationships is that,

$$\Delta E_{\mathrm{sx}}^{\mathrm{sys}} = E_{\mathrm{sx}}^{\mathrm{sys}} - E_{\mathrm{gs}}^{\mathrm{sys}} = \epsilon_l^{\mathrm{ens}} - \epsilon_h^{S_0} \ , \tag{1}$$

i.e., the excitation energy is *exactly* the difference between the ensemble LUMO and ground state HOMO. For the family of ensembles, $\hat{\Gamma}^{\mathrm{sx},w} = (1-w)|S_0\rangle\langle S_0| + w|\mathrm{sx}\rangle\langle \mathrm{sx}|$, we may conveniently re-express eq. (1) as,

$$\Delta E_{\mathrm{sx}}^{\mathrm{sys}} = \epsilon_l^{\mathrm{sx},w} - \epsilon_h^{\mathrm{sx},w=0}, \ \forall \ 0 < w \leq \tfrac{1}{2} \ , \tag{2}$$

where the upper bound ensures that the low energy state is always weighted more than the excited state.[13] Here we recognise that $\hat{\Gamma}^{w=0} = |S_0\rangle\langle S_0|$ is a special case of a pure ground state. Finally, we may take the limit, $w \to 0^+$, of an infinitesmal excitation. As we show below, this limit means that we can bypass additional calculations[24,25] that would otherwise be necessary to compute the ensemble.

Eq. (1) represents the first key result of this work. It is an exact result, despite similarities to recent, successful approximations.[47] It also applies more generally than the illustrative case of a singlet ground state. Firstly, it applies, as given, to systems where the triplet is the ground state and/or where $\frac{1}{\sqrt{2}}[|1^2 \cdots h^{\uparrow} l^{\downarrow}\rangle + |1^2 \cdots h^{\downarrow} l^{\uparrow}\rangle]$ has a lower energy than $|1^2 \cdots h^2\rangle$ – excitation energies simply become negative. Secondly, because the three exact relationships apply to the lowest excitation energy of any system, it may be adapted to ground states with large numbers of unpaired electrons, or spatial degeneracies. In such cases one must identify the correct ensemble, as well as 'h' and 'l' to use in eq. (1) or (2). Section 1 of the SI justifies generalizations, subject to a reasonable postulate.

Let us now turn to approximations. A single excitation ($S_0 \to T_1$ or $S_0 \to S_1$) from

$h \to l$, may be approximated by an EDFA,[25,28]

$$\begin{aligned}\mathcal{E}_{\rm Hxc}^{{\rm sx},w} \approx &(1-w)E_{\rm Hxc}^{\rm DFA}[\rho_{S_0}] + wE_{\rm Hxc}^{\rm DFA}[\rho_{T_1}] \\ &+ \Theta_{S_1} 2w\langle hl|lh\rangle \ , \end{aligned} \tag{3}$$

Here, ρ_{S_0} is the one-body reduced density matrix (1-RDM) of $|S_0\rangle$, and ρ_{T_1} is the 1-RDM of $|T_1\rangle$. The DFA may be of conventional (e.g. PBE[48]), hybrid (e.g. B3LYP[49]) or range-separated hybrid (e.g. ωB97x[50]) form, although the latter is not considered further. The last term in eq. (3) is the singlet-triplet splitting, $2\langle hl|lh\rangle = 2\int \frac{d\boldsymbol{r}d\boldsymbol{r}'}{|\boldsymbol{r}-\boldsymbol{r}'|}\phi_h(\boldsymbol{r})\phi_l^*(\boldsymbol{r}')\phi_l(\boldsymbol{r})\phi_h^*(\boldsymbol{r}')$. Θ_{S_1} indicates that it appears only if one is interested in $S_0 \to S_1$.

The energy is minimized by orbitals obeying,[24]

$$[\hat{h}_0 + \hat{v}_{{\rm Hxc},i}^{{\rm sx},w}]\phi_i^{{\rm sx},w} = \epsilon_i^{{\rm sx},w}\phi_i^{{\rm sx},w} + \sum_{j\neq i}\varepsilon_{ij}^{{\rm sx},w}\phi_j^{{\rm sx},w}, \tag{4}$$

where $\hat{v}_{{\rm Hxc},i}^{{\rm sx},w}\phi_i = \frac{1}{f_i^w}\frac{\delta\mathcal{E}_{\rm Hxc}^{{\rm sx},w}}{\delta\phi_i^*}$, which covers both the ensemble KS and GKS cases. Here, $f_{i<h} = 2$, $f_h = 2-w$ and $f_l = w$ are average occupation factors. The terms ε_{ij} are required to preserve orthogonality. We may, without loss of generality, assume all quantities are real.

As a first step toward a useful approach, consider the potentials, $\hat{v}_{{\rm Hxc},i}$, in the limit $w \to 0^+$. For all orbitals ($i \leq h$) occupied in S_0 we obtain,

$$\hat{v}_{{\rm Hxc},i}^{\rm sx}\phi_i^{\rm sx} = \hat{v}_{\rm Hxc}[\rho_{S_0}]\phi_i^{\rm sx} + O(w) \ , \qquad \forall i \leq h \ , \tag{5}$$

where $\hat{v}_{\rm Hxc} := \frac{\delta E_{\rm Hxc}^{\rm DFA}[\rho_{S_0}]}{\delta\rho_{S_0}}$. We use sx without explicit dependence on w to denote $w \to 0^+$. However, the LUMO, ϕ_l, has a different effective potential. Only the $O(w)$ terms of eq. (3) depend on ϕ_l^*, meaning that $\frac{\delta\mathcal{E}_{\rm Hxc}^{\rm sx}}{\delta\phi_l^*} = w\big\{\hat{v}_{\rm Hxc}^{\rm DFA}[\rho_{T_1}] + \Theta_{S_1}2\hat{v}_{\rm x}[\rho_h]\big\}\phi_l$ where $\hat{v}_{\rm Hxc} := \frac{\delta E_{\rm Hxc}[\rho_{T_1}]}{\delta\rho_{T_1,\uparrow}}$ is the majority spin potential, and $\hat{v}_{\rm x}$ is an exchange operator. But because $f_l = w$ is also

$O(w)$ we obtain,

$$\hat{v}^{\rm sx}_{{\rm Hxc},l}\phi^{\rm sx}_l = \big\{\hat{v}_{\rm Hxc}[\rho_{T_1}] + \Theta_{S_1} 2\hat{v}_{\rm x}[\rho_h]\big\}\phi^{\rm sx}_l + O(w) \; . \tag{6}$$

Therefore, $[\hat{h}_0 + \hat{v}_{\rm Hxc}[\rho_{S_0}]]\phi^{\rm sx}_{i\leq h} = \epsilon^{\rm sx}_i\phi^{\rm sx}_i + \varepsilon^{\rm sx}_{il}\phi^{\rm sx}_l$, and, $[\hat{h}_0 + \hat{v}^{\rm sx}_{{\rm Hxc},l}]\phi^{\rm sx}_l = \epsilon^{\rm sx}_i\phi^{\rm sx}_i + \sum_{i\leq h}\varepsilon^{\rm sx}_{il}\phi^{\rm sx}_i$. Details are in Section 2 of the SI.

Our next step is to make the reasonable[35] assumption that the orbitals, $\phi_{i\leq h}$, change only at $O(w)$. This means that the off-diagonal elements of $\varepsilon^{\rm sx}_{lj}$ must also be $O(w)$ and may be dropped. Consequently, the occupied ($i \leq h$) orbitals obey the *same effective Hamiltonian* as a typical ground state calculation, i.e.,

$$\{\hat{h}_0 + \hat{v}^{S_0}_{\rm Hxc}\}\phi^{S_0}_i = \epsilon^{S_0}_i\phi^{S_0}_i \; , \qquad\qquad \hat{v}^{S_0}_{\rm Hxc} := \hat{v}_{\rm Hxc}[\rho_{S_0}] \; . \tag{7}$$

To determine the LUMO, $\phi^{\rm sx}_l$, we first expand it in terms of virtual orbitals, $a > h$ only, giving $\phi^{\rm sx}_l = \sum_{a>h} U^{\rm sx}_{al}\phi^{S_0}_a$. This ensures it is orthogonal to all occupied orbitals. The LUMO is then described by the lowest orbital energy, $\epsilon^{\rm sx}_l$, and unitary coefficients, U_{al}, obeying,

$$\big\{\epsilon^{S_0}_a\delta_{ab} + [\Delta v_l]^{\rm sx}_{ab}\big\}U^{\rm sx}_{bl} = \epsilon^{\rm sx}_l U^{\rm sx}_{al} \; , \tag{8}$$

where,

$$[\Delta v_l]^{T_1}_{ab} = \int \phi^{S_0\star}_a \{\hat{v}^{T_1}_{\rm Hxc}[\rho_{T_1}] - \hat{v}^{S_0}_{\rm Hxc}[\rho_{S_0}]\}\phi^{S_0}_b d\boldsymbol{r} \; , \tag{9}$$

and $[\Delta v_l]^{S_1}_{ab} = [\Delta v_l]^{T_1}_{ab} + 2\langle ha|bh\rangle$. It is important to recognise that the appearance of ρ_{T_1} in eq. (9) means that eq. (8) must be solved self-consistently, because ρ_{T_1} depends on ϕ_l which depends on $U^{\rm sx}_{al}$. Procedurally, one: i) obtains orbitals and energies for $i \leq h$ from a typical ground state singlet calculation; and ii) afterward obtains $\epsilon^{\rm sx}_l$ by iterating eqs. (8) and (9) to self-consistency – see Section 3 of the SI.

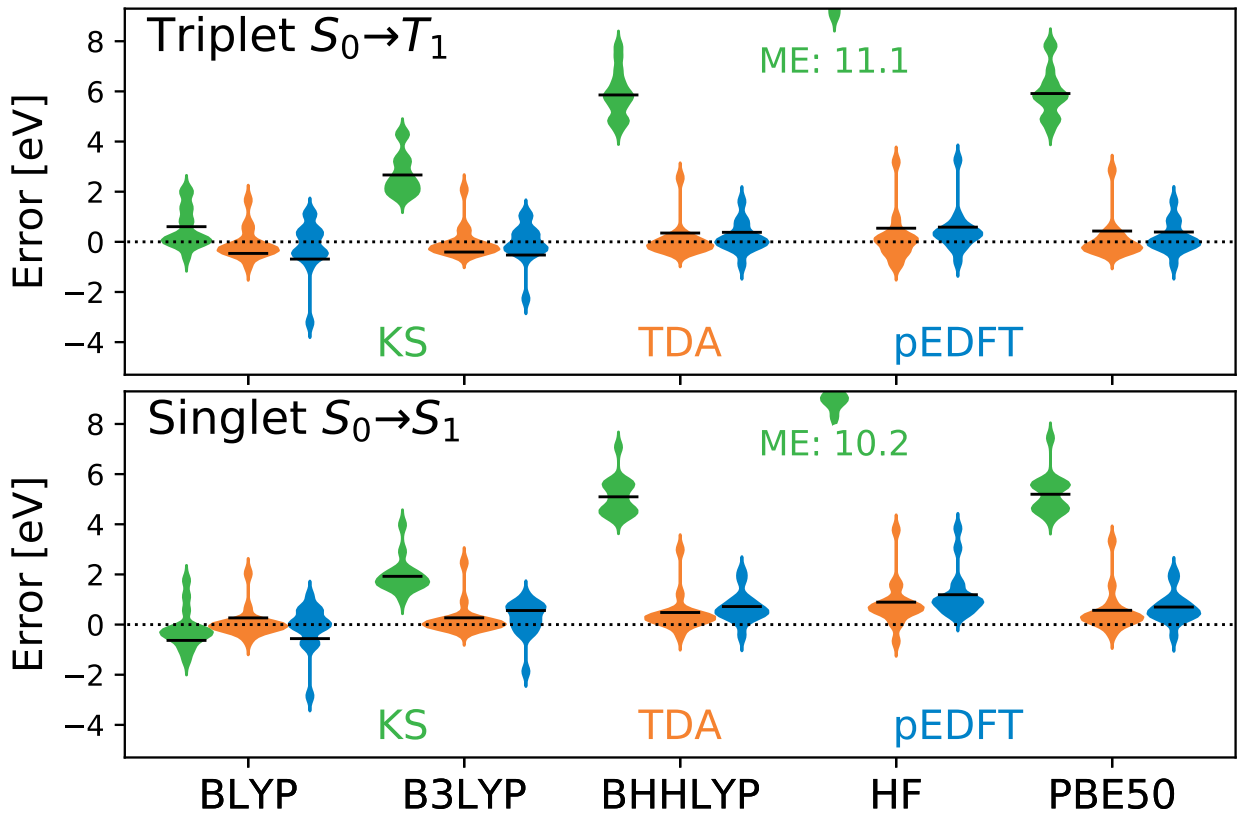

Figure 1: Violin plots showing the distribution of errors across triplet (top) and singlet (bottom) excitations from our test set. Excitations are obtained from KS DFT (green), TDA-TDDFT (orange) and the pEDFT (blue), using a variety of hybrid DFAs. Horizontal bars indicate the mean absolute error, shown as positive numbers when the mean error is positive, and negative otherwise.

Finally, we see the excitation energy is given by,

$$\Delta E_{S_0 \rightarrow T_1 \text{ or } S_1} = \epsilon_l^{T_1 \text{ or } S_1} - \epsilon_h^{S_0} \ , \tag{10}$$

which we denote "perturbative EDFT" (pEDFT) to stress that is obtained in the perturbative limit, $w \rightarrow 0^+$. The pEDFT HOMO-LUMO gap of eq. (10) would be exact if one had access to the exact Hxc functional. As shown below, it offers significant improvements on the regular HOMO-LUMO gap when DFAs are employed.

To assess the accuracy of pEDFT we calculate the the lowest lying $S_0 \rightarrow T_1$ and $S_0 \rightarrow S_1$ transitions from the Loos and co-workers 2018 benchmark set[52] as well as the BeO ground

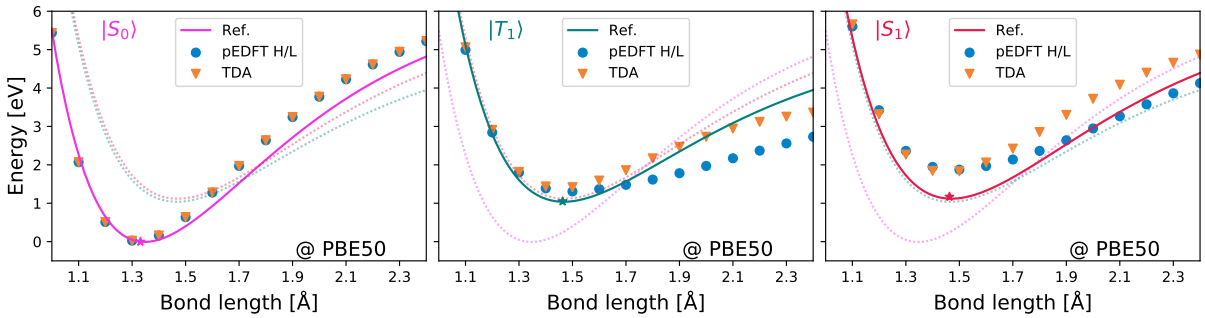

Figure 2: PBE50 potential energy surfaces for low-lying states of BeO, computed using TDA TDDFT (orange triangles) and pEDFT (blue circles). Reference data is shown as solid lines (theory) and stars (experiment[51]). Zero is the optimized $|S_0\rangle$ energy. Pale, dotted curves show other energy surfaces to reveal where level crossing occurs.

state potential energy surface (PES). These examples are chosen due to their difficulty in possessing multiple low lying excited states, or in the case of BeO in reordering of the excited states across the PES. This is to demonstrate that pEDFT can perform well even in typically difficult systems, where other excitation calculation approaches might fail. For comparison we also calculate these transitions using KS orbitals and the Tamm-Dancoff approximation to time-dependent density functional theory (TDA-TDDFT).[53] TDDFT results are computed using ORCA.[54] Technical details are given in Section 4 of SI.

We pay specific attention to the symmetries of the electronic transitions calculated. We note that acquiring the correct transition symmetry, corresponding to the lowest energy excitation, is sometimes not strictly from the HOMO-LUMO gap, for example from HOMO to LUMO+2 instead. Transitions between the highest and lowest orbital of given symmetries are likely to obey a generalization of eq. (1), as discussed in the paragraph between eqs (2) and (3). It is beyond the scope of the present work to resolve whether all such cases have a completely rigorous grounding. Section 4 in the SI provides details of the orbitals that give rise to specific transitions, the transition symmetry, and an accompanying discussion. Thus, in the spirit of practicality for the remainder of this discussion, we simply take them as given.

Concerning ourselves first with the Loos and co-workers benchmark set, we exclude streptocyanine-C1 due to its doublet ground state, leaving us with 17 $S_0 \rightarrow S_1$ transitions

and 16 $S_0 \rightarrow T_1$ transitions. To demonstrate that pEDFT can effectively utilize established DFAs we present results for a variety of hybrid DFAs with different fractions of exact exchange: BLYP[55] (0%), B3LYP[49] (20%), BHHLYP[56] (50%), Hartree-Fock (HF, 100%) and PBE50 (50% HF in PBE0). The collective errors of these transitions for each method are presented in Figure 1 as violin plots. All calculations on the benchmark set are performed using cc-pVDZ[57] basis set.

The primary result from Figure 1 is the similar performance of pEDFT and TDA-TDDFT methods across the spectrum of fractional exact exchange. This comparison validates the use of pEDFT as competitive in terms of accuracy with TDA-TDDFT, using an easy to implement and low cost routine.

The secondary result is that gap opening by HF exchange[31] is completely cancelled by pEDFT. Indeed, results with 50% mixing seem to be optimal. This reflects the fact that the effective potential felt by unoccupied orbitals is corrected within the self-consistency cycle, which ensures that all orbitals are correctly bound.

Finally, twelve of the systems in the benchmark set have singlet and triplet gaps computed using the same excited state symmetries, which lets us compute their singlet triplet splitting energies, $E_{ST} = E_{S_1} - E_{T_1}$. TDDFT gives mean errors of 0.32 (BLYP), 0.33 (B3LYP), 0.38 (BHHLYP), 0.52 (HF) and 0.42 eV (PBE50). pEDFT (using $\epsilon_l^{S_1} - \epsilon_l^{T_1}$) is slightly worse for all DFA except PBE50 and HF, with mean errors of 0.39, 0.40, 0.43, 0.46 and 0.42 eV, respectively.

So far we have focused on fixed geometries. To go beyond this restriction, the PES for BeO is presented in Figure 2. Excited state surfaces in BeO have been the subject of long-standing computational interest.[58] Reference CCSDTQ calculations for the BeO potential energy surfaces are conducted using MRCC.[59] All calculations on BeO are conducted using the aug-cc-pVDZ[57] basis set. A CCSD basis set correction to aug-cc-pvqz is applied to the reference data. pEDFT and TDA-TDDFT results are calculated using PBE50.

Similar performance between pEDFT and TDA-TDDFT is again observed, particularly

the prediction of the Morse potential minima of T_1 and S_1, which are both slightly overestimated. The Morse potential curve of pEDFT is flatter than TDDFT, which places it in worse agreement to the reference for T_1, but better agreement for S_1. Both methods maintain a smooth curve through the rearrangement of excited states, which is a reflection of the stability of both methods, something not many excited state transition calculations (including spin-flip TDA, Supplementary Figure 3) approaches can boast.

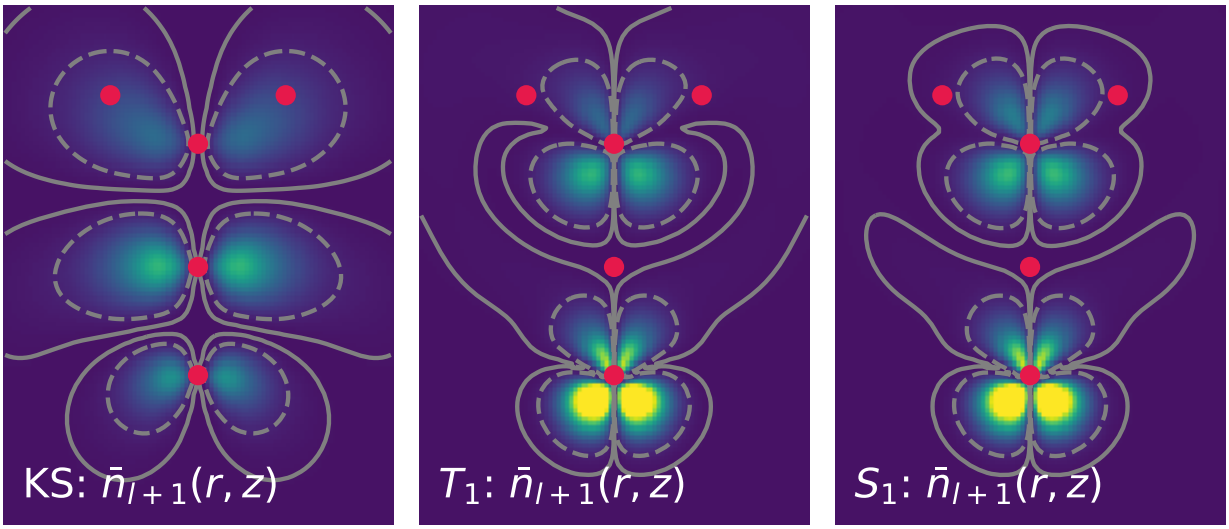

Figure 3: Densities, $n_{l+1} = \phi^2_{l+1}$, of $l+1$ orbitals in ketene averaged around the C-C-O axis. Reports the original KS orbital, (left) as well as orbitals after triplet (T_1, centre) and singlet (S_1, right) pEDFT self-consistency cycles – all for PBE. Solid/dashed lines are $10^{-3}/10^{-2}$ contours.

Finally, let us consider the importance of the pEDFT self-consistency cycle that relaxes the "LUMO" to minimize the excitation energy. All of the excitations reported so far involve transitions between different spatial symmetries, meaning their orbitals change only a little during the pEDFT optimization, as they are "preserved" by the symmetry. However, for the case of ketene the HOMO and LUMO+1 orbitals have the same fundamental symmetry (unlike h and l, used in the benchmark set) and therefore offer more interesting results. Figure 3 shows PBE densities of the $l+1$ orbital, averaged around the C-C-O axis. The pEDFT cycle dramatically changes the density, whether used to compute T_1 or S_1. Less obviously, the singlet and triplet densities are also different – a little more charge moves to

the H atoms in the singlet. Orbital relaxation also reduces the $S_0 \to T_1$ gap by 0.53 eV (to 3.33 eV) and $S_0 \to S_1$ gap by 0.47 eV (to 4.09 eV).

To conclude, we have shown that the "HOMO-LUMO" gap (and generalizations based on symmetries) can be made *exactly equal* to the excitation energy, by defining it carefully in terms of ensemble density functionals using Eq. (1). By taking the limit of infinitesimal interactions it is possible to solve for the gap using a self-consistent cycle only on the LUMO. The resulting energy is rather effective when approximated: it improves conventional HOMO-LUMO gaps significantly, yields similar energies to TDDFT, and is able to describe the potential energy of BeO as well as TDDFT does, and better than spin-flip TDDFT.

Implementation of pEDFT relies only on existing DFA routines, and basic linear algebra operations. Thus, the pEDFT approach may be readily implemented in any quantum chemistry code. The implementation used for the present work is based on `Psi4`[60] and `numpy/scipy` and is available at `https://github.com/stephengdale/pEDFT_HLgap`. Details are given in Section 5 of the SI.

There still remains scope for further improvement. Mostly, the pEDFT gap is of similar quality to its TDDFT counterpart, but there are a few cases (e.g. water) where its quality can be significantly worse. This may be partially explained by a failure to include density-driven correlations[21,22] in Eq. (3), leading to density-driven correlation errors in the resulting energy. Improvements may be possible by devising simple functionals for the density-driven correlation energy. Understanding why orbital-energy-based techniques like that of Chan and Hirao[47] improve excitation energies may offer insights in this regard. This problem remains the topic of ongoing work.

Finally, we did not discuss forces here. However, we note that both $\epsilon_h^{S_0}$ and ϵ_l^{sx} are obtained by variational formulae. Therefore, both should be amenable to Hellmann-Feynman treatment of forces, with the necessary adjustments for basis set incompleteness. We are presently working on implementing forces.

Acknowledgement

This work was supported by the Australian Research Council (DP200100033); the National Computational Merit Allocation Scheme (NCMAS project `ca11`) for National Computational Infrastructure, Australia; and the Griffith high-performance computer, Awoonga. LK is additionally supported by the Aryeh and Mintzi Katzman Professorial chair and the Helen and Martin Kimmel Award for Innovative Investigation.

Supporting Information Available

Includes:

1. Details and generalizations of eq. 1 of the main paper
2. Details of pEDFT derivation
3. Pseudo-code implementation of pEDFT
4. Technical details of calculations, including supplementary figures and tables
5. Description of software

References

(1) Hohenberg, P.; Kohn, W. Inhomogeneous Electron Gas. *Phys. Rev.* **1964**, *136*, B864–B871.

(2) Kohn, W.; Sham, L. J. Self-consistent Equations Including Exchange and Correlation Effects. *Phys. Rev.* **1965**, *140*, A1133–A1138.

(3) Burke, K. Perspective on Density Functional Theory. *J. Chem. Phys.* **2012**, *136*, 150901.

(4) Becke, A. D. Perspective: Fifty Years of Density-functional Theory in Chemical Physics. *J. Chem. Phys.* **2014**, *140*, 18A301.

(5) Jones, R. O. Density Functional Theory: Its Origins, Rise to Prominence, and Future. *Rev. Modern Phys.* **2015**, *87*, 897.

(6) Grimme, S.; Schreiner, P. R. Computational Chemistry: The Fate of Current Methods and Future Challenges. *Ang. Chemie Int'l Ed.* **2018**, *57*, 4170–4176.

(7) Morgante, P.; Peverati, R. The devil in the details: A tutorial review on some undervalued aspects of density functional theory calculations. *Int. J. Quantum Chem.* **2020**, *120*.

(8) Runge, E.; Gross, E. K. Density-functional Theory for Time-dependent Systems. *Phys. Rev. Lett.* **1984**, *52*, 997.

(9) Onida, G.; Reining, L.; Rubio, A. Electronic excitations: density-functional versus many-body Green's-function approaches. *Rev. Mod. Phys.* **2002**, *74*, 601–659.

(10) Ullrich, C. *Time-dependent Density Functional Theory: Concepts and Applications*; Oxford University Press: Oxford, 2012.

(11) Marques, M., Maitra, N. T., Nogueira, F. M., Gross, E. K. U., Rubio, A., Eds. *Fundamentals of Time-dependent Density Functional Theory*; Springer: Berlin, 2012.

(12) Maitra, N. T. Perspective: Fundamental aspects of time-dependent density functional theory. *J. Chem. Phys.* **2016**, *144*, 220901.

(13) Gross, E. K. U.; Oliveira, L. N.; Kohn, W. Rayleigh-Ritz Variational Principle for Ensembles of Fractionally Occupied States. *Phys. Rev. A* **1988**, *37*, 2805–2808.

(14) Gross, E. K. U.; Oliveira, L. N.; Kohn, W. Density-functional Theory for Ensembles of Fractionally Occupied States. I. Basic Formalism. *Phys. Rev. A* **1988**, *37*, 2809–2820.

(15) Yang, Z.-h.; Trail, J. R.; Pribram-Jones, A.; Burke, K.; Needs, R. J.; Ullrich, C. A. Exact and Approximate Kohn-Sham Potentials in Ensemble Density-functional Theory. *Phys. Rev. A* **2014**, *90*, 042501.

(16) Pribram-Jones, A.; Yang, Z.-h.; Trail, J. R.; Burke, K.; Needs, R. J.; Ullrich, C. A. Excitations and Benchmark Ensemble Density Functional Theory for Two Electrons. *J. Chem. Phys.* **2014**, *140*.

(17) Yang, Z.-h.; Pribram-Jones, A.; Burke, K.; Ullrich, C. A. Direct Extraction of Excitation Energies from Ensemble Density-functional Theory. *Phys. Rev. Lett.* **2017**, *119*, 033003.

(18) Deur, K.; Mazouin, L.; Fromager, E. Exact Ensemble Density Functional Theory for Excited States in a Model System: Investigating the Weight Dependence of the Correlation Energy. *Phys. Rev. B* **2017**, *95*, 035120.

(19) Gould, T.; Pittalis, S. Hartree and Exchange in Ensemble Density Functional Theory: Avoiding the Nonuniqueness Disaster. *Phys. Rev. Lett.* **2017**, *119*, 243001.

(20) Deur, K.; Fromager, E. Ground and Excited Energy Levels Can Be Extracted Exactly from a Single Ensemble Density-functional Theory Calculation. *J. Chem. Phys.* **2019**, *150*, 094106.

(21) Gould, T.; Pittalis, S. Density-driven Correlations in Many-electron Ensembles: Theory and Application for Excited States. *Phys. Rev. Lett.* **2019**, *123*, 016401.

(22) Fromager, E. Individual Correlations in Ensemble Density-functional Theory: State-driven/density-driven Decompositions without Additional Kohn-Sham Systems. *Phys. Rev. Lett.* **2020**, *124*, 243001.

(23) Gould, T.; Stefanucci, G.; Pittalis, S. Ensemble Density Functional Theory: Insight from the Fluctuation-dissipation Theorem. *Phys. Rev. Lett.* **2020**, *125*, 233001.

(24) Gould, T.; Kronik, L. Ensemble Generalized Kohn-Sham Theory: The Good, the Bad, and the Ugly. *J. Chem. Phys.* **2021**, *154*, 094125.

(25) Gould, T. Approximately Self-consistent Ensemble Density Functional Theory: Toward Inclusion of All Correlations. *J Phys Chem Lett* **2020**, *11*, 9907–9912.

(26) Loos, P.-F.; Fromager, E. A Weight-dependent Local Correlation Density-functional Approximation for Ensembles. *J. Chem. Phys,* **2020**, *152*, 214101.

(27) Marut, C.; Senjean, B.; Fromager, E.; Loos, P.-F. Weight Dependence of Local Exchange-correlation Functionals in Ensemble Density-functional Theory: Double Excitations in Two-electron Systems. *Faraday Discuss.* **2020**, *224*, 402–423.

(28) Gould, T.; Kronik, L.; Pittalis, S. Double Excitations in Molecules from Ensemble Density Functionals: Theory and Approximations. *Phys. Rev. A* **2021**, *104*, 022803.

(29) Yang, Z. Second-order perturbative correlation energy functional in the ensemble density-functional theory. *Phys. Rev. A* **2021**, *104*, 052806.

(30) Cernatic, F.; Senjean, B.; Robert, V.; Fromager, E. Ensemble Density Functional Theory of Neutral and Charged Excitations. *Top. Curr. Chem.* **2021**, *380*.

(31) Kümmel, S.; Kronik, L. Orbital-dependent Density Functionals: Theory and Applications. *Rev. Modern Phys.* **2008**, *80*, 3–60.

(32) Perdew, J. P.; Ruzsinszky, A.; Constantin, L. A.; Sun, J.; Csonka, G. I. Some Fundamental Issues in Ground-State Density Functional Theory: A Guide for the Perplexed. *J. Chem. Theory Comput.* **2009**, *5*, 902–908.

(33) Baerends, E. J.; Gritsenko, O. V.; van Meer, R. The Kohn–Sham gap, the fundamental gap and the optical gap: the physical meaning of occupied and virtual Kohn–Sham orbital energies. *Phys. Chem. Chem. Phys.* **2013**, *15*, 16408–16425.

(34) Seidl, A.; Görling, A.; Vogl, P.; Majewski, J. A.; Levy, M. Generalized Kohn-Sham Schemes and the Band-gap Problem. *Phys. Rev. B* **1996**, *53*, 3764–3774.

(35) Gould, T.; Toulouse, J. Kohn-Sham Potentials in Exact Density-functional Theory at Noninteger Electron Numbers. *Phys. Rev. A* **2014**, *90*, 050502.

(36) Perdew, J. P.; Parr, R. G.; Levy, M.; Balduz, J. L. Density-functional Theory for Fractional Particle Number: Derivative Discontinuities of the Energy. *Phys. Rev. Lett.* **1982**, *49*, 1691–1694.

(37) Levy, M.; Perdew, J. P.; Sahni, V. Exact Differential Equation for the Density and Ionization Energy of a Many-particle System. *Phys. Rev. A* **1984**, *30*, 2745–2748.

(38) Almbladh, C.-O.; von Barth, U. Exact results for the charge and spin densities, exchange-correlation potentials, and density-functional eigenvalues. **1985**, *31*, 3231–3244.

(39) Gould, T.; Pittalis, S.; Toulouse, J.; Kraisler, E.; Kronik, L. Asymptotic Behavior of the Hartree-exchange and Correlation Potentials in Ensemble Density Functional Theory. *Phys. Chem. Chem. Phys.* **2019**, *21*, 19805–19815.

(40) Cohen, A. J.; Mori-Sanchez, P.; Yang, W. Insights into Current Limitations of Density Functional Theory. *Science* **2008**, *321*, 792–794.

(41) Kraisler, E.; Kronik, L. Piecewise Linearity of Approximate Density Functionals Revisited: Implications for Frontier Orbital Energies. *Phys. Rev. Lett.* **2013**, *110*, 126403.

(42) Kraisler, E.; Kronik, L. Fundamental Gaps with Approximate Density Functionals: The Derivative Discontinuity Revealed from Ensemble Considerations. *J. Chem. Phys.* **2014**, *140*, 18A540.

(43) Kraisler, E.; Kronik, L. Elimination of the Asymptotic Fractional Dissociation Problem

in Kohn-sham Density-functional Theory Using the Ensemble-generalization Approach. *Phys. Rev. A* **2015**, *91*, 032504.

(44) Janak, J. F. Proof That $\partial E/\partial n_i = \epsilon_i$ in Density-functional Theory. *Phys. Rev. B* **1978**, *18*, 7165–7168.

(45) Garrick, R.; Natan, A.; Gould, T.; Kronik, L. Exact Generalized Kohn-Sham Theory for Hybrid Functionals. *Phys Rev X* **2020**, *10*.

(46) Sahni, V.; Massa, L.; Singh, R.; Slamet, M. Quantal Density Functional Theory of Excited States. *Phys. Rev. Lett.* **2001**, *87*, 113002.

(47) Chan, B.; Hirao, K. Rapid Prediction of Ultraviolet–visible Spectra from Conventional (non-time-dependent) Density Functional Theory Calculations. *J. Phys. Chem. Lett.* **2020**, *11*, 7882–7885.

(48) Perdew, J. P.; Burke, K.; Ernzerhof, M. Generalized Gradient Approximation Made Simple. *Phys. Rev. Lett.* **1996**, *77*, 3865–68.

(49) Becke, A. D. A New Mixing of Hartree-Fock and Local Density-functional Theories. *J. Chem. Phys.* **1993**, *98*, 1372–77.

(50) Chai, J.-D.; Head-Gordon, M. Systematic Optimization of Long-range Corrected Hybrid Density Functionals. *J. Chem. Phys.* **2008**, *128*, 084106.

(51) Liu, X.; Truppe, S.; Meijer, G.; Pérez-Ríos, J. The Diatomic Molecular Spectroscopy Database. *J. Cheminform.* **2020**, *12*.

(52) Loos, P.-F.; Scemama, A.; Blondel, A.; Garniron, Y.; Caffarel, M.; Jacquemin, D. A Mountaineering Strategy to Excited States: Highly Accurate Reference Energies and Benchmarks. *J. Chem. Theory Comput.* **2018**, *14*, 4360–4379.

(53) Hirata, S.; Head-Gordon, M. Time-dependent Density Functional Theory within the Tamm–dancoff Approximation. *Chem. Phys. Lett.* **1999**, *314*, 291–299.

(54) Neese, F.; Wennmohs, F.; Becker, U.; Riplinger, C. The Orca Quantum Chemistry Program Package. *The Journal of Chemical Physics* **2020**, *152*, 224108.

(55) Becke, A. D. Density-functional Exchange-energy Approximation with Correct Asymptotic-behavior. *Phys. Rev. A* **1988**, *38*, 3098–100.

(56) Becke, A. D. A New Mixing of Hartree–fock and Local Density-functional Theories. *J. Chem. Phys.* **1993**, *98*, 1372.

(57) Dunning Jr, T. H. Gaussian basis sets for use in correlated molecular calculations. I. The atoms boron through neon and hydrogen. *J. Chem. Phys.* **1989**, *90*, 1007–1023.

(58) Chelikowsky, J. R.; Kronik, L.; Vasiliev, I. Time-dependent density-functional calculations for the optical spectra of molecules, clusters, and nanocrystals. *J. Phys.: Condens. Matt.* **2003**, *15*, R1517–R1547.

(59) Kállay, M.; Nagy, P. R.; Mester, D.; Rolik, Z.; Samu, G.; Csontos, J.; Csóka, J.; Szabó, P. B.; Gyevi-Nagy, L.; Hégely, B. et al. The MRCC Program System: Accurate Quantum Chemistry from Water to Proteins. *J. Chem. Phys.* **2020**, *152*, 074107.

(60) Parrish, R. M.; Burns, L. A.; Smith, D. G.; Simmonett, A. C.; DePrince III, A. E.; Hohenstein, E. G.; Bozkaya, U.; Sokolov, A. Y.; Di Remigio, R.; Richard, R. M. et al. Psi4 1.1: An Open-source Electronic Structure Program Emphasizing Automation, Advanced Libraries, and Interoperability. *J. Chem. Theor. Comput.* **2017**, *13*, 3185.